The Journal of Immunology

Regulation of Sustained Actin Dynamics by the TCR and Costimulation as a Mechanism of Receptor Localization

Irina Tskvitaria-Fuller, Andrew L. Rozelle, Helen L. Yin and Christoph Wülfing

J Immunol 2003; 171:2287-2295; ;
doi: 10.4049/jimmunol.171.5.2287
http://www.jimmunol.org/content/171/5/2287

The Journal of Immunology is published twice each month by
The American Association of Immunologists, Inc.,
1451 Rockville Pike, Suite 650, Rockville, MD 20852

Print ISSN: 0022-1767 Online ISSN: 1550-6606.

Regulation of Sustained Actin Dynamics by the TCR and Costimulation as a Mechanism of Receptor Localization

Irina Tskvitaria-Fuller,* Andrew L. Rozelle,† Helen L. Yin,† and Christoph Wülfing[1]*‡

The localization of receptors, signaling intermediates, and cytoskeletal components at the T cell/APC interface is thought to be a major determinant of efficient T cell activation. However, important questions remain open. What are the dynamics of the T cell cytoskeleton as a potential mediator of such localization? How are they regulated by the TCR and costimulatory receptors? Do they actually mediate receptor localization? In this study, we have addressed these questions. Even under limiting T cell activation conditions, actin accumulated immediately and transiently at the T cell/APC interface, the microtubule organizing center reoriented toward it. In contrast, sustained (>5 min) actin accumulation in highly dynamic patterns depended on an optimal T cell stimulus: high concentrations of the strong TCR ligand agonist peptide/MHC and engagement of the costimulatory receptors CD28 and LFA-1 were required in an overlapping, yet distinct, fashion. Intact sustained actin dynamics were required for interface accumulation of TCR/MHC in a central pattern and for efficient T cell proliferation, as established using a novel approach to selectively block only the sustained actin dynamics. These data suggest that control of specific elements of actin dynamics by TCR and costimulatory receptors is a mechanism to regulate the efficiency of T cell activation. ***The Journal of Immunology*****, 2003, 171: 2287–2295.**

Efficient physiological activation of T cells in a cellular interaction with APCs has two intriguing characteristics, the requirement for the simultaneous engagement of multiple receptors and the localization of signaling and effector functions. 1) Although the engagement of the TCR by peptide/MHC is the key regulator of T cell activation, efficient activation also requires the engagements of costimulatory receptors, in particular of CD28 by B7 and LFA-1 by ICAM-1. This is evident, e.g., in the proliferation of naive T cells where CD28 drives the production of the T cell autocrine growth factor IL-2, and LFA-1 stabilizes the IL-2 mRNA (1, 2). 2) As a well-studied example of the localization of T cell signaling and effector functions, receptor engagement in T cell/APC couples is not only restricted to the T cell/APC interface, but also is often highly organized within the interface. In particular, MHC/peptide/TCR complexes tend to accumulate at the center of the interface, a pattern that is called a complete immunological synapse (3–6). As this pattern is tightly correlated with efficient T cell activation, the localization of receptors and their associated signaling intermediates has been suggested to be a major amplification mechanism in T cell activation (7–10). Interestingly, these two key characteristics of physiological T cell activation, multiple and localized receptor engagement, are linked. The engagement of both TCR and costimulatory receptors regulates the localization of receptors and membrane components (3, 5, 6, 11–13). However, the cellular machinery driving this localization is largely unknown.

The T cell cytoskeleton as the central mediator of cellular organization is likely a key element in subcellular localization. It has been repeatedly suggested that the T cell actin cytoskeleton, because of its organizing role, is a major regulator of T cell signaling and effector functions (7–9, 14). With a description of T cell cytoskeletal dynamics, their regulation by physiological receptor engagement, and their effect of the formation of the immunological synapse, we contribute here to confirming this suggestion. Although it has been established that the T cell cytoskeleton (as judged by filamentous actin (F-actin)[2] distribution and microtubule organizing center (MTOC) orientation) and key regulators (Cdc42 and the Wiskott-Aldrich Syndrome protein (WASP)) are localized at the T cell/APC interface (as recently reviewed in Ref. 15), the dynamics of this polarization, its regulation in T cell/APC couples, and its relevance for receptor localization are unknown. Using fluorescence video microscopy of live, primary T cell/APC couples, we have addressed these questions in this study. Early (<2 min) T cell interface actin accumulation and MTOC localization at the interface constitute the basic T cell cytoskeletal phenotype, as they occur even under limiting activation conditions. Under optimal activation conditions, additional sustained (>5 min) dynamic interface actin accumulation was seen. These sustained actin dynamics were regulated by engagement of CD28, LFA-1, and the TCR in an overlapping but distinct fashion. To investigate the significance of the sustained actin dynamics, we developed a tool that selectively blocked cytoskeletal dynamics associated with optimal, but not limiting, T cell activation, a membrane-permeable version of the C-terminal effector domain of the Wiskott-Aldrich protein (WASP). Using this tool, we showed that intact sustained actin dynamics were required for TCR/MHC accumulation in the central pattern of a complete "immunological synapse" and for efficient T cell proliferation. These data suggest that sustained actin dynamics as regulated by the engagement of the TCR and costimulatory receptors control the formation of the immunological synapse. This likely regulates the efficiency of T cell activation.

*Center for Immunology and Departments of †Physiology and ‡Cell Biology, University of Texas Southwestern Medical Center, Dallas, TX 75390

Received for publication April 10, 2003. Accepted for publication June 30, 2003.

The costs of publication of this article were defrayed in part by the payment of page charges. This article must therefore be hereby marked *advertisement* in accordance with 18 U.S.C. Section 1734 solely to indicate this fact.

[1] Address correspondence and reprint requests to Dr. Christoph Wülfing, Center for Immunology, University of Texas Southwestern Medical Center, 5323 Harry Hines Boulevard, Dallas, TX 75390-9093. E-mail address: christoph.wuelfing@utsouthwestern.edu

[2] Abbreviations used in this paper: F-actin, filamentous actin; MTOC, microtubule organizing center; WASP, Wiskott-Aldrich syndrome protein; GFP, green fluorescent protein; VCA, verprolin, cofilin-homology, acidic; VC, verprolin, cofilin-homology; MCC, moth cytochrome C; DIC, differential interference contrast.

0022-1767/03/$02.00

Materials and Methods

Cells

Properties and handling of primary 5C.C7 TCR transgenic T cells and CH27 and I-E^k-green fluorescent protein (GFP)-transfected A20 APCs have been described before (6).

tat fusion proteins

The WASP verprolin-, cofilin-homology, acidic (VCA) and verprolin cofilin-homology (VC) domains were PCR amplified from a full-length WASP cDNA using the sense primer AGTCACTCGAGTATGGGGGGC CTGGCCCCTGG and the reverse primers AGTCACTCGAGTCAGTCA TCCCATTCATCATC and AGTCACTCGAGTCAGTGGATGGCTCTGC TTCTC, respectively. The domains were expressed in *Escherichia coli* BL21 from a modified pET T7 expression vector (Novagen, Madison, WI) such that the amino acids MGSSHHHHHHGGYGRKKRRERRGGYPY DVPDYASLGGTGHVHICSR were added to the N terminus of the domains containing a histidine purification tag, the HIV tat peptide, and a HA detection tag. They were purified according to Nagahara et al. (16). The identity of the purified proteins was verified by mass spectrometry. As additional control, the tat peptide by itself (YGRKKRRERRRGGSGG) was used.

Microscopy and MHC accumulation analysis

Live primary effector-target cell couples constitute a particular imaging challenge, as the effectors are highly motile, small, and round. T cell-APC cell couple formation is a relatively rare event. GFP labels have to be dim to represent physiological protein levels, thus limiting the dynamic range of the fluorescence data. Cells with <20 fluorescence intensity steps from the least to the most intense pixel were excluded from analysis. Under these circumstances, an image quality equal to fixed cell analysis cannot be achieved. To avoid data misinterpretation, we use exactly defined analysis criteria as described below and blind image analysis to avoid observer bias. The microscopy system and sample handling were the same as before (6). Microscopy and MHC image analysis procedures were the same as in Wülfing et al. (6). T cells were pretreated with 0.5 μM Jasplakinolide (Molecular Probes, Eugene, OR) for 5 min and 0.1 μM Jasplakinolide was present during the T cell/APC interaction. T cells were preincubated with 200 nM tat fusion protein for 30 min at 37°C and 200 nM tat fusion protein were present during the T cell/APC interaction. As the formation of the immunological synapse does not require APC cytoskeletal activity (5, 6, 17), tat WASP VCA uptake into the APC during T cell/APC interactions is not a concern. MHC accumulation patterns were defined as before (6). Briefly, a "central" pattern is defined as a MHC-GFP accumulation at the central (not closer than 20% of the interface diameter to the edge of the interface) 25% of the interface area with a GFP intensity of >40% above the cellular background. A pattern of similar intensity covering the whole interface is called "spread." A central accumulation on the background of a spread one was counted as central, if the fluorescence intensity of the central area as defined above was at least twice as much above the cellular background than the intensity of the accumulation in the rest of the interface.

Retroviral transduction, actin-GFP, and tubulin-GFP analysis

β-actin-GFP and β5-tubulin-GFP (18, 19) were expressed from a Moloney murine leukemia virus-derived retroviral expression vector (20) containing an additional internal phosphoglycerol kinase promoter or not, respectively. T cells were primed on day 0 with lymph node APCs plus 3 μM moth cytochrome C (MCC) peptide, retrovirally transduced as described in Costa et al. (20) on day 1, FACS sorted on day 5, and used for microscopy between days 7 and 9. Actin-GFP or tubulin-GFP-positive cells were purified by FACS. Actin-GFP and tubulin-GFP image acquisition and image analysis were performed as for MHC accumulation with the following modifications. Three-dimensional reconstructions were made at all time points up to 3 min after T cell activation and at selected time points thereafter. In actin-GFP analysis, a lamellopodial actin accumulation was defined as an actin-GFP intensity of >50% above the cellular background at both leading edges of the interface and not >40% above the cellular background at the rest of the interface. Sustained accumulation (>5 min after interface formation) was scored as an actin-GFP intensity of >100%, between 40 and 100%, or <40% (see none in Fig. 2*B*) at the area of accumulation (irrespective of the geometrical pattern) above the intensity of an area of the same size on the cellular background. In rare cases where interface actin accumulation was continuous with noninterface accumulation, the cell couple was excluded from analysis, as actin accumulation was not unambiguously induced by the interface. A central pattern was defined as for the MHC-GFP accumulation (see also Fig. 1*B*). A peripheral pattern was defined as an actin-GFP accumulation in a ring fragment of ≥270° around the outer part of the interface at >40% of the cellular background together with an fluorescence intensity at the central area of the interface (as defined above) that is less than half of the ring fluorescence intensity (see Fig. 1*B*). For analysis of the three-dimensional tubulin-GFP data, a cell was counted as having a well-defined MTOC, when in a three-dimensional reconstruction the top 25% of the fluorescence intensity were contained in <25% of the T cell diameter parallel and perpendicular to the direction of cell movement or the interface. The position of the MTOC was determined by dividing the T cell into three sections of equal length along the cellular axis parallel to the direction of cell movement (excluding the uropod because of its greatly varying length) or perpendicular to the interface. If the MTOC as defined above was fully contained within one of the sections it was scored 1, 2, or 3 with increasing distance form the leading edge of the T cell or the interface. If the MTOC was positioned on one of the internal section boundaries it was scored 1.5 or 2.5, respectively.

Staining of fixed T cell/APC couples

After 15 min of T cell/APC interactions at 37°C, cells were fixed and stained as in Monks et al. (3). Texas Red-conjugated phalloidin (Molecular Probes) was used at 1 U per cover slip. I-E^k-transfected A20 cells were used as APCs to allow unambiguous distinction between T cells and APCs. Data were acquired as three-dimensional data sets for the GFP and Texas Red-conjugated phalloidin data and a single differential interference contrast (DIC) image similar to MHC accumulation experiments. Productive T cell/APC couples were identified by a tight T cell/APC interface with flattening of the APC surface at the interface. Phenotypes were classified as in the actin-GFP experiments. T cell F-actin concentration was several-fold higher than that of the APCs allowing the unambiguous assignment of interface F-actin to the T cell.

Proliferation assays

5C.C7 T cell proliferation was assayed by ^{3}[H]thymidine uptake as described (21).

Results

Actin dynamically accumulates at the T cell/APC interface

As a first step to investigate cytoskeletal dynamics in T cell/APC interactions, we characterized the T cell actin cytoskeleton in the interaction of live, primary 5C.C7 T cells with activating APCs in real time using a retrovirally expressed actin-GFP fusion protein (Fig. 1). Actin-GFP fusion proteins are widely used to visualize cytoskeletal dynamics and have been used successfully in the interaction of Jurkat T cells with Ab-coated coverslips (22, 23). The 5C.C7 TCR recognizes the MCC peptide 88–103 presented by I-E^k. Therefore, we used I-E^k-expressing B cell lymphoma cells incubated with MCC peptide as APCs. Initially, we characterized T cell actin dynamics in response to an optimal T cell stimulus, i.e., a high concentration of agonist peptide/MHC on the APC surface and access of the key costimulatory receptors CD28 and LFA-1 to their APC ligands B7 and ICAM-1 (Fig. 2*A*). In our analysis, we distinguish an early (<2 min after T cell/APC couple formation, Fig. 2*B*) and a sustained (>5 min, Fig. 2*C*) stage of T cell activation.

Early, all T cells showed actin accumulation at the interface (Fig. 2*B*), 76% in a specific biphasic sequence of patterns. First, the interface widened with the most prominent actin accumulation being at two opposing edges of the interface, a pattern called "lamellopodial accumulation" here (at the 0:40 min-time point in Fig. 1, *A* and *C*, supplemental movies S1 and S2).[3] This pattern is reminiscent of the annular actin distribution observed in Jurkat T cells that spread on anti-TCR Ab-coated coverslips (22, 23). Second, the interface contracted slightly accompanied by actin patterns that cover the interface more evenly (at the 1:00 min time

[3] The on-line version of this article contains supplemental material.

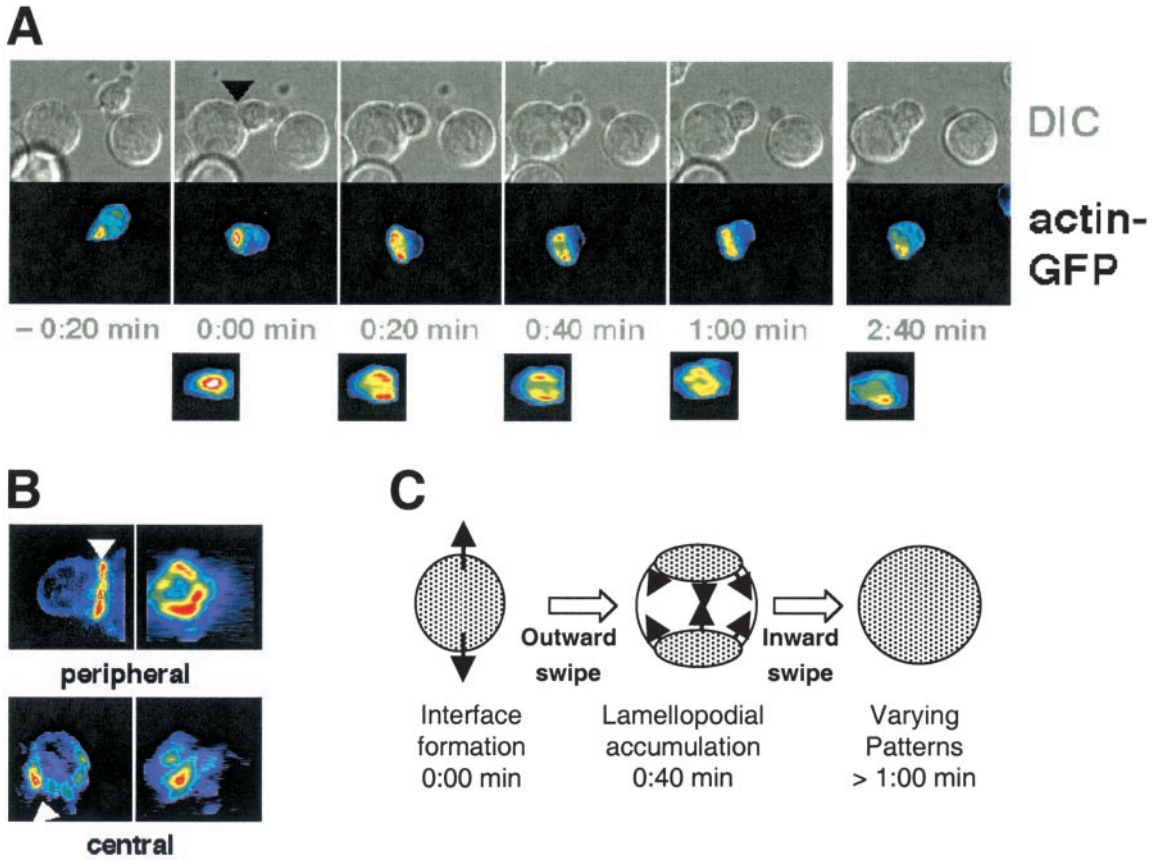

FIGURE 1. Actin accumulation at the T cell/APC interface. *A,* An interaction of an actin-GFP transduced 5C.C7 T cells with a CH27 B cell lymphoma APC under optimal conditions (Fig. 2*A*) is shown. As labeled on the *right*, in the *top row* of each panel, DIC images (cell couple formation is marked with a black arrowhead) are shown; in the *middle*, matching top-down projections of three-dimensional actin-GFP fluorescence data are shown. At the *bottom* (under the designation of the time points), projections of the actin-GFP data are given where the T cell has been rotated to show a frontal view of the interface. The actin-GFP fluorescence intensity is displayed in a false color rainbow scale (increasing from blue to green, yellow, red, and white). T cell activation (t = 0:00 min) induced immediate actin accumulation at the T cell/APC interface, followed by lamellopodial actin accumulation (t = 0:40 min) and subsequent slight interface contraction with actin distribution at varying locations throughout the interface. The images are individual frames from movie S1. *B,* F-actin staining of two T cell/APC couples is shown. Only the T cells are shown completely and are centered within the images. The two cells represent peripheral and central F-actin accumulation as indicated. For each cell, two projections of the three-dimensional data are shown. On the *left* are top-down projections (similar to the *middle panels* in *A*). Small parts of the APCs can be seen at the *right* (peripheral) and the *bottom left* (central). White arrowheads denote the T cell/APC interface. On the *right*, frontal views of the interface (similar to the *bottom panels* is *A*) are shown. The phalloidin fluorescence intensity is encoded as in *A*. *C,* The double-swiping motion is illustrated. A schematic representation of a frontal view of the interface (as used in the bottom row in *A*) is given with shading indicating areas where the most prominent actin accumulation can occur. Black arrows depict the swiping directions, the first of which moves actin to opposing edges of the interface (to create the lamellopodial accumulation, *middle panel*), the second one moves part of the actin back to the center. Although the formation of the lamellopodial pattern is a stereotypical sequence of events, its dissolution leads to a large variety of different patterns.

point in Fig. 1, *A* and *C*, supplemental movies S1 and S2). The formation and dissolution of the lamellopodial pattern is reminiscent of an outward inward double "swiping motion" (Fig. 1*C*) and is referred to here as such. The time scale of the initial accumulation of receptors at the T cell/APC interface (4–6, 17) is the same as that of the actin swiping motion described here, suggesting that the actin motion might corral receptor/ligand couples as a mediator of early receptor accumulation. This is consistent with a recent three-dimensional analysis of TCR motion that established the need for cellular machinery to rapidly move membrane mass and TCR molecules toward the interface within the first minute after cell couple formation (24).

After the initial swiping motion, actin remained accumulated covering varying areas within the entire interface. In the sustained stage (≥5 min after cell couples formation), 86% of the T cell/APC couples (Fig. 2*C*) still showed actin accumulation at the interface. The patterns were highly dynamic (supplemental movies S1 and S2) and ranged from preferential actin accumulation at the center to preferential accumulation at the periphery of the T cell/APC interface (Figs. 1*B* and 2*D*).

As an actin-GPF fusion protein visualizes the distribution of both monomeric and F-actin, we separately investigated the localization of polymerized actin by staining fixed T cell/APC couples with phalloidin (Fig. 1*B*). Corroborating the actin-GFP data, we found actin accumulation at the T cell/APC interface in 85% of the T cell/APC couples in a variety of patterns ranging from central to peripheral (Figs. 1*B* and 2*E*). Similar F-actin accumulation at the T cell/APC interface has also been described previously (14, 25–27). Small differences between actin-GFP and F-actin staining phenotypes are discussed in the supplementary material.

In summary, with an optimal T cell stimulus, actin accumulated dynamically at the T cell/APC interface. This started with a distinct double-swiping motion suggestive of early receptor/ligand corralling. It continued in a highly dynamic fashion in a large variety of patterns indicative of continuous actin turnover at the T cell/APC interface.

A

	TCR signal	Costimulation	Inhibitors
Optimal T cell stimulus	10 μM MCC [1]	no blocking antibodies	none
Costimulation blockade	10 μM MCC [1]	anti-B7 to block CD28 engagement anti-ICAM to block LFA-1	none
Weak TCR signal	0.1 μM MCC [2]	no blocking antibodies	none
Limiting T cell stimulus	0.1 μM MCC [2]	anti-B7 to block CD28 engagement anti-ICAM to block LFA-1	none
Blocked actin dynamics	10 μM MCC [1]	no blocking antibodies	200 nM tat WASP VCA 0.5 μM Jasplakinolide [3]

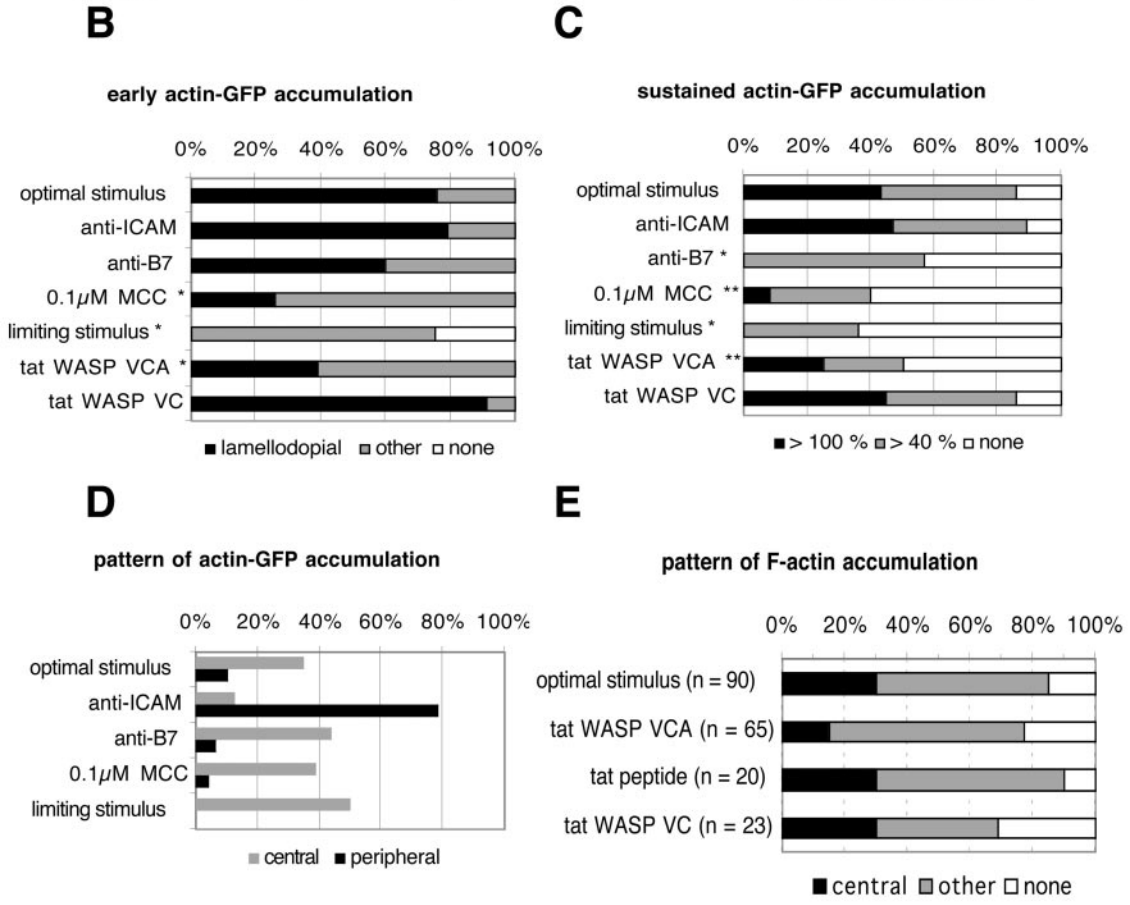

FIGURE 2. Regulation of T cell actin dynamics. *A*, Experimental conditions in the investigation of the regulation of cytoskeletal dynamics are listed. [1], MCC denotes MCC (82–103). [2],The reduced agonist peptide concentration is achieved as 10 μM of a 1/100 dilution of MCC into the null peptide MCC D93E,K99T,T102S. [3], T cells were pretreated with 0.5 μM Jasplakinolide and only 0.1 μM was present during microscopy. *B*, The percentage of T cell/APC couples showing lamellopodial actin-GFP accumulation (Fig. 1*A*) within the first minute after cell couple formation, a different pattern of actin accumulation, or no actin accumulation is given under the conditions indicated (*A*). ∗, A significant ($p < 0.01$) difference in the percentage of cell couples showing lamellopodial actin accumulation vs optimal stimulus. Twenty to 43 cell couples (on average 23) from at least four independent experiments were analyzed per condition. Only 12 cell couples could be analyzed under limiting conditions, as T cell activation was rare. *C*, The percentage of cell couples showing sustained T cell actin-GFP accumulation at >100%, at between 40 and 100%, and at <40% above cellular background (none) is given under the conditions indicated (*A*). ∗ or ∗∗, A significant ($p < 0.05$ and $p < 0.005$, respectively) difference in the percentage of cell couples showing no actin accumulation vs optimal stimulus. Analysis statistics were as in *B*. *D*, The percentage of cell couples showing central or peripheral actin-GFP accumulation, respectively, at least once during the observation period of >5 min is given under the conditions indicated (*A*). Analysis statistics were as in *B*. *E*, The percentage of T cell/APC couples with F-actin accumulation at the T cell/APC interface in a central pattern (Fig. 1*B*), in any other pattern, or without accumulation is given under the conditions denoted. The number of cell couples analyzed is given in parentheses. The reduction in the percentage of cell couples showing central F-actin accumulation in the presence of tat WASP VCA vs optimal stimulus is significant with $p < 0.05$. Differences in the percentages of cells showing no F-actin accumulation are not significant. Each experiment has been performed at least three times.

The lamellopodial pattern of early actin accumulation and occurrence and patterns of sustained actin accumulation were differentially regulated by TCR, CD28, and LFA-1 engagement

To investigate the physiological regulation of T cell cytoskeletal dynamics, we studied it with less than optimal T cell stimuli. We blocked engagement of CD28 and LFA-1 with Abs to their ligands B7 and ICAM-1, respectively, and/or decreased the concentration of the strong TCR ligand agonist peptide-MHC by 100-fold to the minimal concentration necessary to activate 5C.C7 T cells (Ref. 6; Fig. 2*A*). Under all conditions, the formation of tight T cell/APC couples could still be observed.

As assayed with actin-GFP, early T cell actin accumulation occurred in ≥75% of the cell couples under all conditions (Fig. 2*B*). However, the specific sequence of patterns of the double-swiping

motion was dependent on a high concentration of agonist peptide/MHC. At 100-fold reduced concentrations of agonist peptide/MHC, only 26% of the T cell-APC couples showed the double-swiping motion as opposed to 76% under optimal conditions ($p < 0.01$).

The amount of sustained actin accumulation was substantially reduced using less than optimal stimuli. Under limiting conditions (Fig. 2*A*), in the absence of CD28 engagement, or in the presence of a 100-fold reduced concentration of agonist peptide-MHC, the percentage of cell couples without sustained actin accumulation was significantly ($p < 0.05$) increased (from 11% under optimal conditions to 64, 43, and 60%, respectively) (Fig. 2*C*). Under the same three conditions, 0, 0, and 8% of the cell couples showed sustained actin accumulation at >100% of the cellular background as opposed to 43% under optimal conditions. Interestingly under all these conditions, the lack of sustained actin accumulation correlates with reduced TCR-MHC accumulation (Ref. 6; Fig. 7).

To evaluate the highly dynamic patterns of actin accumulation, we determined in which percentage of the T cell-APC couples the two most extreme patterns, all actin accumulation at the center of the interface (central) or all actin accumulation at the edge of the interface (peripheral; similar to Fig. 1*B*), occurred at least once. LFA-1 engagement was required for actin accumulation at the center of the interface. In the presence of blocking Abs to the LFA-1 ligand ICAM-1, 78% of the cell couples showed peripheral and 13% central actin accumulation at least once as opposed to 10% peripheral and 35% central accumulation under optimal conditions. This reduction in central actin accumulation correlates with less central TCR-MHC accumulation (6). Interestingly, the effects of CD28 engagement on the patterns of actin vs TCR/MHC/PKCθ accumulation (4, 6, 28) did not correlate. CD28 engagement was only required for central accumulation of the latter. This suggests that factors in addition to patterning of actin dynamics, possibly differential receptor/ligand size, contribute to the patterns of receptor localization.

In summary early, T cell actin accumulated at the T cell-APC interface even under limiting activation conditions. A high concentration of the strong TCR ligand agonist peptide/MHC was required for the double-swiping motion that is possibly involved in early receptor corralling. In the sustained phase, a high concentration of agonist peptide/MHC was required for continued actin accumulation. Engagement of the principal costimulatory receptors CD28 and LFA-1 was also necessary for sustained actin accumulation and its central pattern, respectively. The different phenotypes of TCR, CD28, or LFA-1 engagement suggest that these receptors have distinct functions in the regulation of actin dynamics.

Rapid MTOC reorientation toward the T cell/APC interface is an inherent feature of even limiting T cell activation

As an indicator of T cell polarity, we next visualized the T cell MTOC in the interaction of live, primary 5C.C7 T cells with activating APCs in real time using a retrovirally expressed tubulin-GFP fusion protein (19). Initially, we used an optimal T cell stimulus (Fig. 2*A*). Irrespective of T cell morphology, the interface with the APC formed at the part of the T cell surface that was opposite the MTOC (80% of the cell couples, $n = 34$). Subsequently, the MTOC rapidly reoriented toward the T cell/APC interface (Figs. 3 and 4*A*, supplemental movie S3). Sixty-three percent of the cell couples ($n = 41$) had completed the reorientation within 1 min of interface formation. The MTOC moved at a rate of 4.5 ± 2.5 μm/min. Subsequently, the MTOC remained localized at the T cell/APC interface. These data corroborate earlier observations using modulated polarization microscopy and staining of fixed T cell/APC couples with anti-tubulin Abs (26, 27, 29–32).

To study the regulation of MTOC localization, we analyzed the dynamics of MTOC reorientation toward the interface and the percentage of cell couples showing a well-defined MTOC (*Materials and Methods*). Treatment with 100 nM Nocodazole showed that MTOC definition (Fig. 4*B*) was a feature of intact microtubule dynamics. Of all conditions tested, only a limiting T cell stimulus showed a small defect in MTOC localization. The initial reorientation of the MTOC toward the interface was delayed (Fig. 4*A*), the MTOC position at the final time point was significantly ($p < 0.005$) farther from the interface than under optimal conditions (1.19 vs 1.00), and the percentage of cell couples showing a well-defined MTOC at the final time point was slightly but significantly ($p < 0.05$) reduced (95–79%). However, this defect was minor as 63% of the cell couples under limiting activation conditions still displayed a well-defined MTOC located at the center of the interface. Rapid MTOC reorientation toward the interface thus was robust even under limiting T cell activation conditions. It is an inherent feature of T cell activation.

Intact actin dynamics are required for the accumulation of TCR/MHC at the center of the interface and for efficient T cell proliferation

The parallel regulation of both TCR/MHC accumulation (6) and sustained T cell actin dynamics by engagement of the TCR and costimulatory receptors suggests that these receptors could regulate TCR/MHC accumulation by controlling actin dynamics. To directly address this hypothesis, we needed a tool to selectively interfere with actin dynamics associated with optimal T cell activation while actin dynamics associated with limiting activation

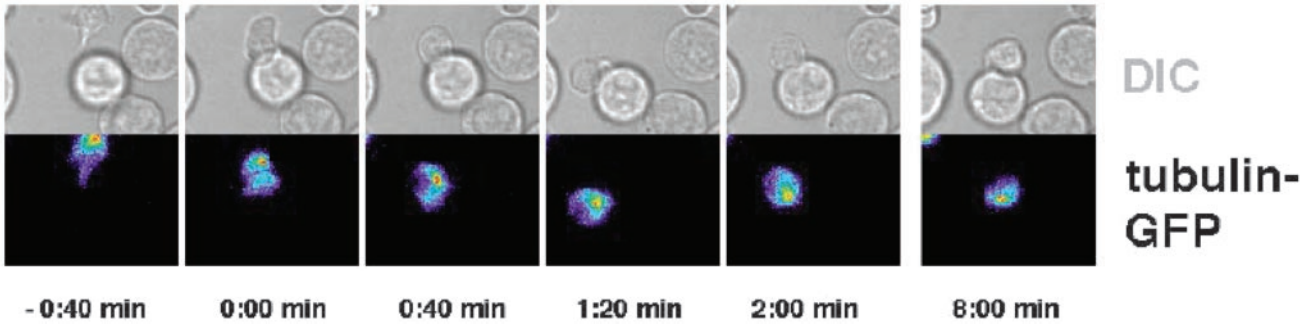

FIGURE 3. MTOC reorientation toward the T cell/APC interface. An interaction of a tubulin-GFP-transduced 5C.C7 T cells with CH27 B cell lymphomas is shown similar to Fig. 1. The MTOC is visible as the location of highest tubulin-GFP fluorescence intensity. Although located at the posterior end of the T cell before interface formation ($t \leq 0$ min), it swings around toward the interface within 2 min and remains there. The images are individual frames from supplemental movie S3.

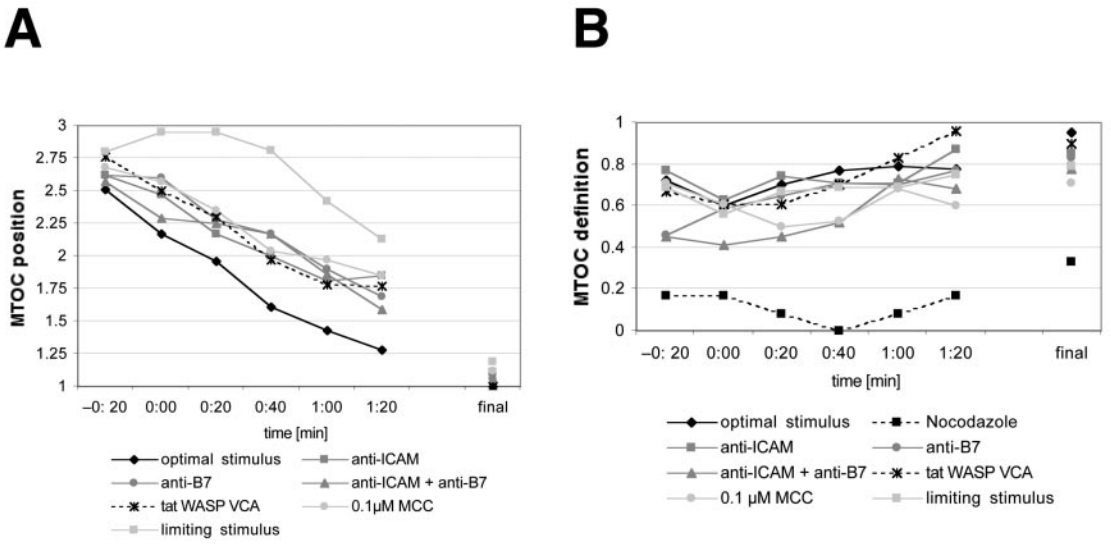

FIGURE 4. Regulation of MTOC localization. *A*, The average position of the MTOC is plotted against time under the denoted conditions (Fig. 2*A*). The final time point is at least 5 min after interface formation. A MTOC position of 1 is closest to, and a position of 3 is furthest from, the interface (see *Materials and Methods*). MTOC orientation is significantly delayed under limiting conditions ($p < 0.005$ for difference in MTOC location against optimal stimulus at time points 0:00 to 1:20 min). Twenty to 48 cell couples (on average 26, only 16 under limiting conditions as T cell activation was rare) from at least five independent experiments were analyzed per condition. *B*, The percent of cell couples showing a well-defined MTOC (see *Materials and Methods*) is plotted against time as in *A*. Only 100 nM Nocodazole interfered significantly ($p < 0.01$ for all time points) with the formation of a well-defined MTOC. Analysis statistics are as in *A*.

remained intact. Commonly used pharmacological inhibitors of actin dynamics, e.g., cytochalasin D, drastically interfere with salient features of limiting T cell activation, such as cell couple formation and interface tightness (17). To achieve a less drastic and, therefore, physiologically more meaningful block of actin dynamics, we targeted the Arp2/3 complex as a key regulator of actin polymerization. It is activated by binding of the VCA domain of activated WASP family proteins (33–36). Expression of an isolated VCA domain interferes with localized actin polymerization (33–35, 37). Therefore, we used the WASP VCA domain as an inhibitor of actin dynamics. Controls and domain properties are discussed in more detail in the supplementary material.

We introduced tat WASP VCA into the primary T cells as tat fusion protein (supplementary material and Refs. 16 and 38). At a concentration of 200 nM, tat WASP VCA specifically interfered with T cell actin dynamics to the desired extent. Early T cell actin accumulation at the T cell/APC interface was consistently observed. However, its lamellopodial pattern (Fig. 2*B*), the extent of sustained actin accumulation (Fig. 2*C*), and the central pattern of F-actin accumulation (Fig. 2*E*) were partially yet significantly blocked (Fig. 5 and more detail in the supplementary material). These data are consistent with published results showing that Jurkat T cell actin accumulation at an interface with an anti-CD3 Ab-coated bead is suppressed by the scar VCA domain (37). As a corroborating approach to interfere with actin dynamics, we blocked F-actin depolymerization with a small concentration of Jasplakinolide (*Materials and Methods*) (39, 40). A similar yet slightly more drastic interference with actin dynamics was found (supplementary material) (41).

Next, we used tat WASP VCA and Jasplakinolide to ask whether sustained actin dynamics are required for TCR/MHC accumulation. TCR/MHC accumulation at the center of the T cell/APC interface is the hallmark of a complete immunological synapse as associated with efficient T cell activation, whereas noncentral accumulation patterns are found under a much wider range of activation conditions (as recently reviewed in Ref. 10). We used an I-E^k-GFP fusion protein to visualize MHC/peptide/TCR complexes (6). tat WASP VCA and Jasplakinolide treatment interfered significantly ($p < 0.05$) with the central TCR-MHC accumulation. Only 29 and 13% of the T cell-APC couples showed central TCR-MHC accumulation in the presence of tat WASP VCA and Jasplakinolide as opposed to 59% under optimal conditions (Table I). Interestingly, while the occurrence of the central

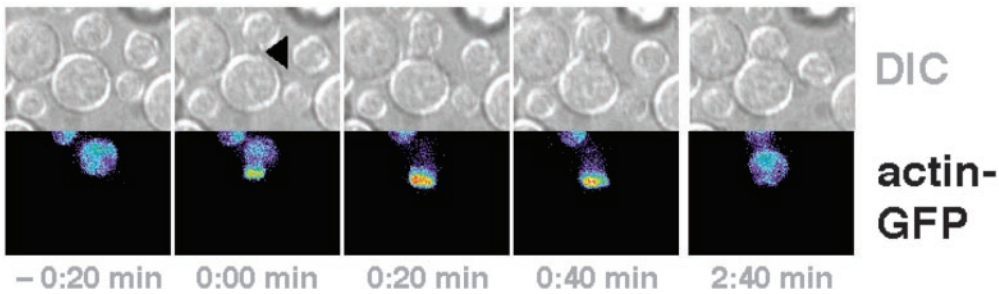

FIGURE 5. tat WASP VCA interferes with T cell cytoskeletal dynamics. T cell actin-GFP in a T cell/APC interaction (as in Fig. 1) is shown in the presence of 200 nM tat WASP VCA. The initial actin swiping motion and sustained actin accumulation at the T cell/APC interface are missing.

Table I. *Intact actin dynamics are required for central TCR/MHC accumulation*

Condition	Pattern of TCR/MHC Accumulation[a] Central (%)	Spread (%)	Amount[c] (%)	None (%)	n^b
Optimal stimulus	59	22	1.9	20	96 (11)
200 nM tat WASP VCA	29*	65*	1.9	6*	34 (3)
200 nM tat WASP VC	41	34	1.8	24	29 (3)
0.5 μM Jasplakinolide	13**	88**	3.5**	0**	24 (3)

[a] Phenotypes as defined in *Materials and Methods.*
[b] Number of cell couples analyzed in number of independent experiments.
[c] Percentage of the total MHC on the APC surface that has been translocated to the interface at 3:20 min after cell couple formation as calculated in (6); (25 cell couples on average per condition, 18 minimum) significance of differences against optimal stimulus is indicated by asterisks (*, $p < 0.05$; **, $p < 0.005$).

pattern was substantially disturbed, the extent of TCR/MHC accumulation was unchanged or enhanced (Table I). TCR/MHC accumulation patterns associated with an incomplete immunological synapse are thus not dependent on sustained actin dynamics. This might well be the consequence of differential receptor translocation mechanisms for central and noncentral patterns (as discussed elsewhere (10)). In addition, fewer T cell/APC couples without any significant TCR/MHC accumulation were observed in the presence of tat WASP VCA or Jasplakinolide (Table I), possibly indicative of less TCR/MHC removal from the interface. In both observations, Jasplakinolide interfered with TCR/MHC dynamics more strongly than tat WASP VCA, consistent with its stronger interference with actin dynamics. These data suggest that intact sustained actin dynamics are required for the formation of a complete immunological synapse.

The correlation between central TCR/MHC accumulation and efficient T cell activation suggests that factors governing central TCR/MHC accumulation such as the sustained actin dynamics could also be required for efficient T cell activation. To test this hypothesis, we measured 5C.C7 T cell proliferation in the presence of tat WASP VCA and Jasplakinolide. Despite effective T cell/APC clustering during the proliferation assay (data not shown and consistent with the microscopically observed formation of tight cell couples, Fig. 5 and Ref. 41), Jasplakinolide and tat WASP VCA both interfered with T cell proliferation (Fig. 6). Staining for T cell DNA contents with Hoechst 33342 showed that treated T cells did not enter the cell cycle (supplementary material). This suggests that the proliferation defect was caused by an impaired stimulus to divide, consistent with an incomplete formation of the

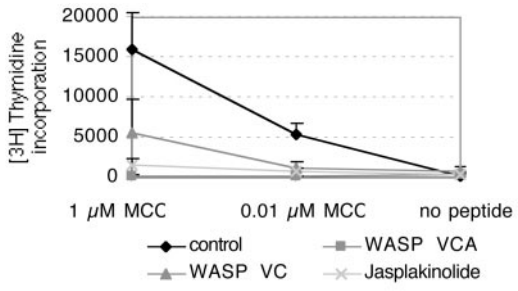

FIGURE 6. Intact sustained actin dynamics are required for efficient T cell proliferation. Proliferation of naive 5C.C7 T cells induced by the indicated concentration of MCC agonist peptide and irradiated splenocytes in the presence of 200 nM tat WASP VCA, 200 nM tat WASP VC, 100 nM Jasplakinolide, or buffer only is shown in cpm incorporated ^{3}[H]thymidine. Similar results were obtained for the proliferation of IL-2-starved primed 5C.C7 T cells stimulated with MCC peptide and mitomycin C-treated CH27 B cell lymphoma cells (data not shown). One representative of three assays is shown.

immunological synapse. Although the control domain tat WASP VC partially blocked T cell proliferation (Fig. 6), even 500 μM of the tat peptide by itself did not block T cell proliferation (data not shown). This is consistent with the suggestion that the G-actin binding ability of the tat WASP VC domain prevents it from being functionally neutral (as further discussed in the supplementary material). However, the partial inhibition of T cell proliferation caused by 200 nM tat WASP VC correlated with a small (statistically not significant) inhibition of central TCR/MHC accumulation (Table I), further supporting a link between complete immunological synapse formation and downstream T cell activation. In summary, specific interference with actin dynamics associated with an optimal but not with a limiting T cell stimulus blocked TCR/MHC accumulation in a central pattern and T cell proliferation. This suggests that intact sustained T cell actin dynamics and the receptors governing it may regulate the efficiency of T cell activation by controlling the formation of a complete immunological synapse.

Discussion

The localization of signaling and effector functions in T cells during their activation by APCs has been suggested to be a major component in the regulation of the efficiency of T cell activation. In this study, we have characterized T cell cytoskeletal dynamics as a mediator of such localization, investigated their regulation, and addressed their relevance. In conjunction with previous studies using the same T cell/APC combination, this provides a picture of a highly dynamic and tightly regulated T cell polarization as summarized in Fig. 7. Early (<2 min after cell couple formation), MTOC reorientation and actin accumulation were observed even under limiting activation conditions. They thus constitute the basic cytoskeletal machinery of T cell activation. In contrast, sustained (≥5 min after cell couple formation) actin accumulation and a long range actin translocation (12) were dependent on the engagement of TCR, CD28, and LFA-1. They thus constitute the part of the cytoskeletal machinery associated with more efficient T cell activation. A high concentration of the strong TCR ligand agonist peptide/MHC and engagement of CD28 and LFA-1 have overlapping yet distinct effects (Fig. 7*B*), thus constituting three elements required for complete T cell cytoskeletal dynamics. CD28 and LFA-1 have been suggested to enhance T cell activation either by facilitation of TCR engagement or as independent signaling receptors. We suggest that costimulatory signaling contributes to the regulation of the actin dynamics for two reasons. First, the distinct actin phenotypes observed for reduced TCR, CD28, or LFA-1 engagement are very difficult to reconcile with a sole role of CD28 and LFA-1 as enhancers of TCR signaling. Why for example would the effects of blocking CD28 engagement and a smaller concentration of agonist peptide/MHC have a very similar effect

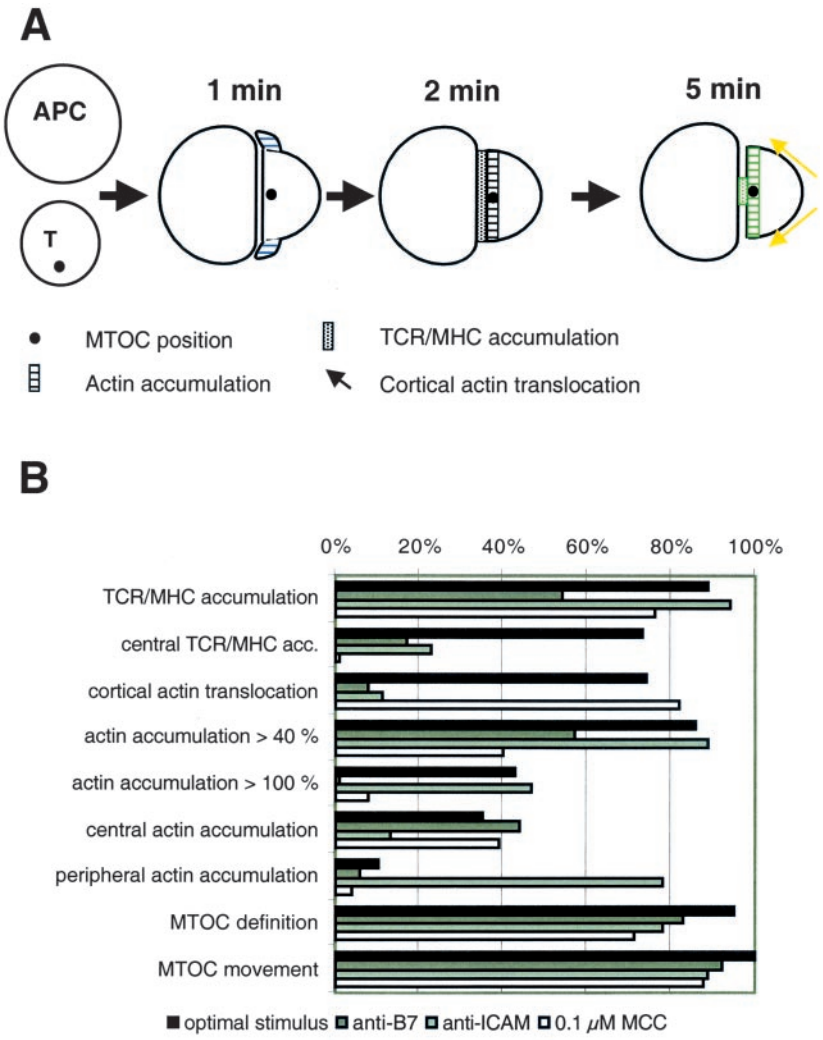

FIGURE 7. Summary of T cell cytoskeletal dynamics. *A*, Elements of T cell polarization (in relation to the formation on the T cell/APC interface as set to $t = 0$ min) are represented as denoted in the lower part of the figure. TCR/MHC accumulation (6) and cortical actin translocation (12) have been described previously. MTOC position and actin accumulation are described here. The regulation of particular phenotypes is color-encoded. Regulation by a strong TCR signal is denoted in blue, regulation by costimulation in yellow, regulation by both in green. Black denotes invariable elements of even limiting T cell activation. *B*, The percentage of T cell/APC couples showing the denoted element of T cell cytoskeletal dynamics under the indicated conditions (Fig. 2*A*) is given. The percentages of cell couples showing TCR/MHC accumulation, TCR/MHC accumulation in a central pattern >5 min after formation of the T cell/APC interface, or translocation of the T cell cortical actin cytoskeleton were determined previously (6, 12). The percentage of cell couples displaying particular actin accumulation phenotypes is directly taken from Fig. 2. The percentage of cell couples displaying a well-defined MTOC, or a MTOC at the center of the interface (as the endpoint of successful MTOC movement) >5 min after interface formation is derived from Fig. 4. The figure demonstrates overlapping, yet distinct, regulation of cytoskeletal dynamics by the TCR, CD28, and LFA-1.

on sustained actin accumulation yet opposite ones (Figs. 2*B* and 7*B*) on the early lamellopodial accumulation and the long range actin translocation? Second, CD28 and LFA-1 engagement by their ligands in isolation directly regulate actin dynamics (42, 43). It thus seems reasonable to assume that they exert the same function in the context of a T cell/APC interaction. Possible mediators of CD28 and LFA-1 signal transduction are phosphatidylinositol 3-kinase (44, 45) and phospholipase Cγ (46).

The parallel regulation of TCR/MHC accumulation and cytoskeletal polarization by TCR and costimulation, indirect evidence derived from signaling studies (7–9), and modeling (47) all point toward a role of the actin cytoskeleton in the formation of the immunological synapse. In this study, we have addressed this directly. With the tat peptide-linked WASP VCA domain we have developed a tool to specifically block those elements of actin dynamics that require an optimal T cell stimulus while leaving those intact that occur under limiting activation conditions. Using this tool we have shown that the accumulation of TCR/MHC couples at the center of the T cell/APC interface, the hallmark of a complete immunological synapse, but not accumulation in other patterns, was dependent on actin dynamics associated with optimal T cell activation. This not only directly confirms the suspected involvement of actin dynamics in the formation of the immunological synapse, but also identifies the specific elements of actin dynamics and synapse structure involved. Possible mechanisms underlying this selectivity are discussed elsewhere (10). As we have also shown that costimulation and TCR engagement regulate these elements of actin dynamics, the data suggest that costimulation and TCR regulate the formation of a complete immunological synapse by controlling T cell actin dynamics. Consistent with the suggested role of a complete immunological synapse as a mediator of efficient T cell activation, we have also shown that intact sustained actin dynamics are required for efficient T cell proliferation. The regulation of the localization of receptors and associated signaling intermediates by controlling actin dynamics thus likely is a major determinant of the efficiency of T cell activation.

Acknowledgments

We thank Roger Sciammas, Gina Costa, and Gary Nolan for help in establishing tat fusions and the retroviral transduction; Beat Imhof for the actin-GFP and tubulin-GFP constructs; Augustin Sanchez for peptide synthesis; and Angela Mobley for expert FACS support. We thank Matthew F. Krummel, Ben Freiberg, Iwona Stroynowski, David Farrar, and Michael K. Rosen for helpful discussions.

References

1. Yashiro, Y., X. G. Tai, K. Toyo-oka, C. S. Park, R. Abe, T. Hamaoka, M. Kobayashi, S. Neben, and H. Fujiwara. 1998. A fundamental difference in the capacity to induce proliferation of naive T cells between CD28 and other costimulatory molecules. *Eur. J. Immunol. 28:926.*
2. Zuckerman, L. A., L. Pullen, and J. Miller. 1998. Functional consequences of costimulation by ICAM-1 on IL-2 gene expression and T cell activation. *J. Immunol. 160:3259.*

3. Monks, C. R., B. A. Freiberg, H. Kupfer, N. Sciaky, and A. Kupfer. 1998. Three-dimensional segregation of supramolecular activation clusters in T cells. *Nature 395:82*.
4. Krummel, M. F., M. D. Sjaastad, C. Wülfing, and M. M. Davis. 2000. Differential clustering of CD4 and CD3ζ during T cell recognition. *Science 289:1349*.
5. Grakoui, A., S. K. Bromley, C. Sumen, M. M. Davis, A. S. Shaw, P. M. Allen, and M. L. Dustin. 1999. The immunological synapse: a molecular machinery controlling T cell activation. *Science 285:221*.
6. Wülfing, C., C. Sumen, M. D. Sjaastad, L. C. Wu, M. L. Dustin, and M. M. Davis. 2002. Costimulation and endogenous MHC ligands contribute to T cell recognition. *Nat. Immunol. 3:42*.
7. Acuto, O., and D. Cantrell. 2000. T cell activation and the cytoskeleton. *Annu. Rev. Immunol. 18:165*.
8. Dustin, M. L., and A. C. Chan. 2000. Signaling takes shape in the immune system. *Cell 103:283*.
9. Krawczyk, C., and J. M. Penninger. 2001. Molecular motors involved in T cell receptor clusterings. *J. Leukocyte Biol. 69:317*.
10. Wülfing, C., I. Tskvitaria-Fuller, N. J. Burroughs, M. D. Sjaastad, J. Klem, and J. D. Schatzle. 2002. Interface accumulation of receptor/ligand couples in lymphocyte activation: methods, mechanisms, and significance. *Immunol. Rev. 189:64*.
11. Viola, A., S. Schroeder, Y. Sakakibara, and A. Lanzavecchia. 1999. T lymphocyte costimulation mediated by reorganization of membrane microdomains. *Science 283:680*.
12. Wülfing, C., and M. M. Davis. 1998. A receptor/cytoskeletal movement triggered by costimulation during T cell activation. *Science 282:2266*.
13. Bromley, S. K., A. Iaboni, S. J. Davis, A. Whitty, J. M. Green, A. S. Shaw, A. Weiss, and M. L. Dustin. 2001. The immunological synapse and CD28-CD80 interactions. *Nat. Immunol. 2:1159*.
14. Fuller, C. L., V. L. Braciale, and L. E. Samelson. 2003. All roads lead to actin: the intimate relationship between TCR signaling and the cytoskeleton. *Immunol. Rev. 191:220*.
15. Cannon, J. L., and J. K. Burkhardt. 2002. The regulation of actin remodeling during T cell-APC conjugate formation. *Immunol. Rev. 186:90*.
16. Nagahara, H., A. M. Vocero-Akbani, E. L. Snyder, A. Ho, D. G. Latham, N. A. Lissy, M. Becker-Hapak, S. A. Ezhevsky, and S. F. Dowdy. 1998. Transduction of full-length TAT fusion proteins into mammalian cells: TAT-p27^{Kip1} induces cell migration. *Nat. Med. 4:1449*.
17. Wülfing, C., M. D. Sjaastad, and M. M. Davis. 1998. Visualizing the dynamics of T cell activation: ICAM-1 migrates rapidly to the T cell:B cell interface and acts to sustain calcium levels. *Proc. Natl. Acad. Sci. USA 95:6302*.
18. Ballestrem, C., B. Wehrle-Haller, and B. A. Imhof. 1998. Actin dynamics in living mammalian cells. *J. Cell Sci. 111:1649*.
19. Ballestrem, C., B. Wehrle-Haller, B. Hinz, and B. A. Imhof. 2000. Actin-dependent lamellipodia formation and microtubule-dependent tail retraction control-directed cell migration. *Mol. Biol. Cell 11:2999*.
20. Costa, G. L., J. M. Benson, C. M. Seroogy, P. Achacoso, C. G. Fathman, and G. P. Nolan. 2000. Targeting rare populations of murine antigen-specific T lymphocytes by retroviral transduction for potential application in gene therapy for autoimmune disease. *J. Immunol. 164:3581*.
21. Wülfing, C., A. Bauch, G. R. Crabtree, and M. M. Davis. 2000. The vav exchange factor is an essential regulator in actin-dependent receptor translocation to the lymphocyte-antigen-presenting cell interface. *Proc. Natl. Acad. Sci. USA 97:10150*.
22. Bunnell, S. C., V. Kapoor, R. P. Trible, W. Zhang, and L. E. Samelson. 2001. Dynamic actin polymerization drives T cell receptor-induced spreading: a role for the signal transduction adaptor LAT. *Immunity 14:315*.
23. Borroto, A., D. Gil, P. Delgado, M. Vicente-Manzanares, A. Alcover, F. Sanchez-Madrid, and B. Alarcon. 2000. Rho regulates T cell receptor ITAM-induced lymphocyte spreading in an integrin-independent manner. *Eur. J. Immunol. 30:3403*.
24. Moss, W. C., D. J. Irvine, M. M. Davis, and M. F. Krummel. 2002. Quantifying signaling-induced reorientation of T cell receptors during immunological synapse formation. *Proc. Natl. Acad. Sci. USA 99:15024*.
25. Ryser, J. E., E. Rungger-Brandle, C. Chaponnier, G. Gabbiani, and P. Vassalli. 1982. The area of attachment of cytotoxic T lymphocytes to their target cells shows high motility and polarization of actin, but not myosin. *J. Immunol. 128:1159*.
26. Sedwick, C. E., M. M. Morgan, L. Jusino, J. L. Cannon, J. Miller, and J. K. Burkhardt. 1999. TCR, LFA-1, and CD28 play unique and complementary roles in signaling T cell cytoskeletal reorganization. *J. Immunol. 162:1367*.
27. Stowers, L., D. Yelon, L. J. Berg, and J. Chant. 1995. Regulation of the polarization of T cells toward antigen-presenting cells by Ras-related GTPase CDC42. *Proc. Natl. Acad. Sci. USA 92:5027*.
28. Huang, J., P. F. Lo, T. Zal, N. R. Gascoigne, B. A. Smith, S. D. Levin, and H. M. Grey. 2002. CD28 plays a critical role in the segregation of PKCθ within the immunologic synapse. *Proc. Natl. Acad. Sci. USA 99:9369*.
29. Kuhn, J. R., and M. Poenie. 2002. Dynamic polarization of the microtubule cytoskeleton during CTL-mediated killing. *Immunity. 16:111*.
30. Kupfer, A., and S. J. Singer. 1989. Cell biology of cytotoxic and helper T cell functions: immunofluorescence microscopic studies of single cells and cell couples. *Annu. Rev. Immunol. 7:309*.
31. Serrador, J. M., J. L. Alonso-Lebrero, M. A. del Pozo, H. Furthmayr, R. Schwartz-Albiez, J. Calvo, F. Lozano, and F. Sanchez-Madrid. 1997. Moesin interacts with the cytoplasmic region of intercellular adhesion molecule-3 and is redistributed to the uropod of T lymphocytes during cell polarization. *J. Cell Biol. 138:1409*.
32. Ratner, S., W. S. Sherrod, and D. Lichlyter. 1997. Microtubule retraction into the uropod and its role in T cell polarization and motility. *J. Immunol. 159:1063*.
33. Blanchoin, L., K. J. Amann, H. N. Higgs, J. B. Marchand, D. A. Kaiser, and T. D. Pollard. 2000. Direct observation of dendritic actin filament networks nucleated by Arp2/3 complex and WASP/Scar proteins. *Nature 404:1007*.
34. Machesky, L. M., and R. H. Insall. 1998. Scar1 and the related Wiskott-Aldrich syndrome protein, WASP, regulate the actin cytoskeleton through the Arp2/3 complex. *Curr. Biol. 8:1347*.
35. Rohatgi, R., L. Ma, H. Miki, M. Lopez, T. Kirchhausen, T. Takenawa, and M. W. Kirschner. 1999. The interaction between N-WASP and the Arp2/3 complex links Cdc42-dependent signals to actin assembly. *Cell 97:221*.
36. Yarar, D., W. To, A. Abo, and M. D. Welch. 1999. The Wiskott-Aldrich syndrome protein directs actin-based motility by stimulating actin nucleation with the Arp2/3 complex. *Curr. Biol. 9:555*.
37. Krause, M., A. S. Sechi, M. Konradt, D. Monner, F. B. Gertler, and J. Wehland. 2000. Fyn-binding protein (Fyb)/SLP-76-associated protein (SLAP), Ena/vasodilator-stimulated phosphoprotein (VASP) proteins and the Arp2/3 complex link T cell receptor (TCR) signaling to the actin cytoskeleton. *J. Cell Biol. 149:181*.
38. Wadia, J. S., and S. F. Dowdy. 2002. Protein transduction technology. *Curr. Opin. Biotechnol. 13:52*.
39. Bubb, M. R., A. M. Senderowicz, E. A. Sausville, K. L. Duncan, and E. D. Korn. 1994. Jasplakinolide, a cytotoxic Natureal product, induces actin polymerization and competitively inhibits the binding of phalloidin to F-actin. *J. Biol. Chem. 269:14869*.
40. Cramer, L. P. 1999. Role of actin-filament disassembly in lamellipodium protrusion in motile cells revealed using the drug Jasplakinolide. *Curr. Biol. 9:1095*.
41. Wülfing, C., B. Purtic, J. Klem, and J. D. Schatzle. 2003. Stepwise cytoskeletal polarization as a series of checkpoints in innate but not adaptive cytolytic killing. *Proc. Natl. Acad. Sci. USA 100:7767*.
42. Porter, J. C., M. Bracke, A. Smith, D. Davies, and N. Hogg. 2002. Signaling through integrin LFA-1 leads to filamentous actin polymerization and remodeling, resulting in enhanced T cell adhesion. *J. Immunol. 168:6330*.
43. Kaga, S., S. Ragg, K. A. Rogers, and A. Ochi. 1998. Stimulation of CD28 with B7-2 promotes focal adhesion-like cell contacts where Rho family small G proteins accumulate in T cells. [Published erratum appears in *1999 J. Immunol. 162:3104.*] *J. Immunol. 160:24*.
44. Prasad, K. V., Y. C. Cai, M. Raab, B. Duckworth, L. Cantley, S. E. Shoelson, and C. E. Rudd. 1994. T-cell antigen CD28 interacts with the lipid kinase phosphatidylinositol 3-kinase by a cytoplasmic Tyr^{P}-Met-Xaa-Met motif. *Proc. Natl. Acad. Sci. USA 91:2834*.
45. Truitt, K. E., C. M. Hicks, and J. B. Imboden. 1994. Stimulation of CD28 triggers an association between CD28 and phosphatidylinositol 3-kinase in Jurkat T cells. *J. Exp. Med. 179:1071*.
46. Kanner, S. B., L. S. Grosmaire, J. A. Ledbetter, and N. K. Damle. 1993. β_2-integrin LFA-1 signaling through phospholipase C-γ1 activation. *Proc. Natl. Acad. Sci. USA 90:7099*.
47. Burroughs, N. J., and C. Wülfing. 2002. Differential segregation in a cell:cell contact interface-the dynamics of the immunological synapse. *Biophys. J. 83:1784*.